

Patrick J. Shamberger · Michael O. Garcia

Geochemical modeling of magma mixing and magma reservoir volumes during early episodes of Kīlauea Volcano's Pu'u 'Ō'ō eruption

Received: 25 March 2005 / Accepted: 16 March 2006 / Published online: 12 July 2006
© Springer-Verlag 2006

Abstract Geochemical modeling of magma mixing allows for evaluation of volumes of magma storage reservoirs and magma plumbing configurations. A new analytical expression is derived for a simple two-component box-mixing model describing the proportions of mixing components in erupted lavas as a function of time. Four versions of this model are applied to a mixing trend spanning episodes 3–31 of Kilauea Volcano's Puu Oo eruption, each testing different constraints on magma reservoir input and output fluxes. Unknown parameters (e.g., magma reservoir influx rate, initial reservoir volume) are optimized for each model using a non-linear least squares technique to fit model trends to geochemical time-series data. The modeled mixing trend closely reproduces the observed compositional trend. The two models that match measured lava effusion rates have constant magma input and output fluxes and suggest a large pre-mixing magma reservoir (46 ± 2 and 49 ± 1 million m^3), with little or no volume change over time. This volume is much larger than a previous estimate for the shallow, dike-shaped magma reservoir under the Puu Oo vent, which grew from ~ 3 to ~ 10 – 12 million m^3 . These volumetric differences are interpreted as indicating that mixing occurred first in a larger, deeper reservoir before the magma was injected into the overlying smaller reservoir.

Keywords Geochemistry · Hawai'i · Kilauea · Magma chamber · Magma mixing · Modeling

Editorial responsibility: D. Dingwell

Electronic Supplementary Material Supplementary material is available at <http://dx.doi.org/10.1007/s00445-006-0074-5> and is accessible for authorized users.

P. J. Shamberger · M. O. Garcia (✉)
Department Geology and Geophysics,
University of Hawaii,
1680 East-West Rd.,
Honolulu, HI 96822, USA
e-mail: mogarcia@soest.hawaii.edu
Tel.: +1-808-9566641
Fax: +1-808-9565521

Introduction

The Pu'u 'Ō'ō eruption, the longest (>22 years) and most intensely studied historic eruption of Kīlauea Volcano (see selected bibliography in Heliker and Mattox 2003), has led to an improved understanding of Hawaiian shield-stage magmatic processes. A high resolution geochemical time-series from the early stages of this eruption (episodes 1–31) documents a period of mixing between an initial hybrid magma, formed by mixing two pockets of magma during episode 1, and new MgO-rich magma (Garcia et al. 1989, 1992). During this period, the magma storage system served as a buffer allowing the composition of the erupted lavas to progressively transition towards the MgO-rich end member (Garcia et al. 1992). The magnitude of this buffering effect, as indicated by the rate of compositional change recorded in the time-series data, should correlate with the volume of the reservoir relative to the input and output fluxes (e.g., Albarède 1993; Pietruszka and Garcia 1999). Thus, when interpreted in the context of a specific mixing model, the well-documented history of lava compositions and effusion rates for the Pu'u 'Ō'ō eruption may offer insight into its shallow-level magmatic plumbing system.

Modeling of geochemical data provides a useful tool for understanding a variety of geological processes (e.g., Broecker 1974; Faure 1986; Albarède 1995), and its value has been well demonstrated in volcanology (Hildreth and Moorbath 1988; Hawkesworth et al. 2004). Geochemical modeling complements geophysical techniques as a means of calculating magma reservoir size and flux rates (e.g., Pietruszka and Garcia 1999). In particular, residence time analysis employs the rate of compositional change in a magmatic system to solve for a characteristic residence time, τ , which is defined as the mass of a steady-state magma reservoir divided by its mass flux rate (Albarède 1993). An analytical expression is derived here describing the proportions of end-member mixing components in the reservoir (and consequently in the erupted lavas) as a function of initial reservoir volume, input and output fluxes, and time. This formulation is based on the same

mass balance constraints used to develop residence time analysis, but differs from previous work in which the box-mixing model is solved explicitly for the ratio of two incompatible elements in the reservoir at any time (e.g., Albarède 1993). In contrast, our solution is more general, allowing the relative proportions of end-member components to be independently calculated by various means, including major and trace element ratios, isotope ratios, and linear mass balance calculations. The derived expression is applied to a geochemical time-series of early Pu'u 'Ō'ō lavas in an attempt to recreate the mixing trend. Model results allow us to evaluate magmatic system characteristics that are difficult to constrain by other methods (e.g., the input flux as a function of time and the minimum volume of initial hybrid magma involved in the mixing). Most Pu'u 'Ō'ō basaltic lavas are very fluid, especially near their vent (Heliker and Mattox 2003). Thus, we can ignore the effects of chaotic fluid mixing processes in our modeling, which are important in highly viscous, silicic systems (e.g., Flinders and Clemens 1996; Perugini et al. 2003).

Eruption summary

The Pu'u 'Ō'ō eruption began on 3 Jan 1983 from a fissure extending from Napau crater nearly 8 km down rift. This eruption was triggered by the intrusion of a dike from Kīlauea's upper east rift zone (Wolfe et al. 1987). Initial lavas were shown to represent hybrids from mixing two rift zone-stored, differentiated magmas (Garcia et al. 1989). During episodes 2 and 3 (25 Feb to 9 Apr 1983), activity was localized to a 1 km length fissure, and the early hybrid magma was erupted chiefly from Pu'u Halulu, originally referred to as the 1123 vent (Wolfe et al. 1988). The Pu'u 'Ō'ō vent also erupted lavas during episodes 2 and 3 and was the dominant vent for subsequent episodes until episode 48 in mid-1986. The composition of Pu'u 'Ō'ō vent lavas from 1983–1985 reflects mixing between two end members: (1) the initial hybrid magma created during episode 1, and (2) a high CaO/TiO₂, MgO-rich new magma (Garcia et al. 1992). By episode 31, no chemical or petrographic signs of mixing are evident and the erupted lavas are thought to consist entirely of the new MgO-rich component. Within this trend, systematic intra-episodic variations in MgO content (lower initial MgO, followed by high MgO) indicate chemical zonation within the shallow magma reservoir, resulting from olivine fractionation and accumulation (Garcia et al. 1992). This effect is most pronounced in episodes 5–10, as well as 30 and 31.

Surface deformation studies conducted during episodes 22–42 suggest that on average, the shallow Pu'u 'Ō'ō magma reservoir is a narrow dike, ~3 m wide, ~1.6 km long and ~2.5 km high (Hoffmann et al. 1990). This study estimated that the shallow reservoir increased from ~3 million m³ to a volume of at least 10–12 million m³ during episodes 3–10. This reservoir is presently linked to the summit reservoir through a 3–4-km-deep conduit, pre-

sumably formed from the initial dike of MgO-rich magma that propagated down-rift (Wolfe et al. 1987).

Two component magma mixing model

The simplest conceptual model of a magma chamber is the standard box model (e.g., Albarède 1995). This model consists of a single, compositionally homogeneous reservoir (Fig. 1), into which magma is injected (Q^{in}), and from which magma is either erupted (Q^{out}) or fractionated (Q^{xtal}). All fluxes (Q) are in units of mass per time. We adopt the box model and consider a single abrupt change in input magma composition; that is, after the start of mixing (t^{onset}), the composition of input magma (magma B) is distinct from the initial reservoir composition (magma A). This model leads to a steady dilution of magma A in the reservoir that is a function of both mass fluxes of magma and the initial reservoir size. A solution to this formulation arises from mass balance considerations which require that

$$\frac{dM}{dt} = Q^{\text{in}} - Q^{\text{out}} - Q^{\text{xtal}} \quad (1)$$

where $M=M(t)$ is the mass of magma in the reservoir as a function of time. A similar constraint may be placed on the mass of magma A (M_A) in the reservoir:

$$\frac{dM_A}{dt} = Q^{\text{in}} X_A^{\text{in}} - Q^{\text{out}} X_A^{\text{out}} - Q^{\text{xtal}} X_A^{\text{xtal}} \quad (2)$$

X_A^{in} , X_A^{out} and X_A^{xtal} are the mass fractions of magma A in the input, output, and fractionated solids, respectively. From the assumptions stated above, the input flux is composed entirely of magma B ($X_A^{\text{in}} = 0$), and the output flux is representative of the homogeneous reservoir composition ($X_A^{\text{out}} = X_A^{\text{res}}$), where X_A^{res} is the mass fraction of magma A in the reservoir. Since $M_A = M X_A^{\text{res}}$, the time derivative of M_A is:

$$\frac{dM_A}{dt} = \frac{d(M X_A^{\text{res}})}{dt} = M \frac{dX_A^{\text{res}}}{dt} + X_A^{\text{res}} \frac{dM}{dt} \quad (3)$$

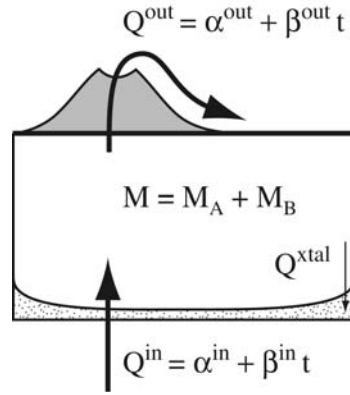
Equating Eqs. (2) and (3) and substituting in Eq. (1), we obtain:

$$M \frac{dX_A^{\text{res}}}{dt} = -Q^{\text{in}} X_A^{\text{res}} + Q^{\text{xtal}} (X_A^{\text{res}} - X_A^{\text{xtal}}) \quad (4)$$

When crystal fractionation is insignificant relative to magma input and output, the mass flux of crystal fractionation can be ignored (this assumption is evaluated below). For this case,

$$\frac{d \ln (X_A^{\text{res}})}{dt} = \frac{-Q^{\text{in}}}{M} \quad (5)$$

Fig. 1 Conceptual diagram for the standard box-model magma chamber including a compositionally homogeneous reservoir, and input (Q^{in}), output (Q^{out}), and crystal fractionation (Q^{xtal}) mass fluxes. Linear input and output fluxes, and negligible crystal fractionation ($Q^{\text{xtal}} \ll Q^{\text{in}}$) are assumed for Pu'u 'Ō'ō. Magma in the chamber (M) is a mixture of magmas A and B (M_A and M_B). Other terms are defined in the text



volume) is this difference between the two fluxes ($\frac{dM}{dt} = \alpha^{\text{in}} - \alpha^{\text{out}}$) and the integrated solution to Eq. (6) is:

$$X_A^{\text{res}}(t) = \exp \left\{ \frac{-\beta t}{\alpha^{\text{in}} - \alpha^{\text{out}}} + \frac{\beta M^o - \alpha^{\text{in}}(\alpha^{\text{in}} - \alpha^{\text{out}})}{(\alpha^{\text{in}} - \alpha^{\text{out}})^2} \right. \\ \left. \times \ln \left(\frac{(\alpha^{\text{in}} - \alpha^{\text{out}})t + M^o}{M^o} \right) \right\} \quad (8)$$

Both time independent (model 2a) and dependent (model 2b) versions are considered below.

The right-hand side of this expression is equal to $-1/\tau$ where τ is the characteristic time for the rate of change of X_A^{res} derived from residence time analysis (Albarède 1993). Integrating Eq. (5) over time and substituting in the time-integrated form of Eq. (1), leads to a general solution:

$$X_A^{\text{res}}(t) = \exp \left\{ \int_0^t \frac{-Q^{\text{in}}}{M^o + \int_0^{t'} (Q^{\text{in}} - Q^{\text{out}} - Q^{\text{xtal}}) dt''} dt' \right\} \quad (6)$$

where M^o is the initial mass of the reservoir. If magmas A and B have the same density, Eq. (6) has a volumetric equivalent where M^o is the initial volume of the reservoir and Q^i is the volumetric flux of component i .

Specific solutions may be found by defining the flux functions, Q^i . For simplicity, input and output fluxes are restricted to linear functions of time ($Q^i = \alpha^i + \beta^i t$) where α and β are independent variables, and Q^{xtal} is assumed to be negligible. In the first model, the volume of the magma reservoir remains constant with time, so the input and output fluxes are equal ($Q^{\text{in}} = Q^{\text{out}} = \alpha + \beta t$). Solving Eq. (6) for constant reservoir volume yields:

$$X_A^{\text{res}}(t) = \exp \left\{ -\frac{\beta}{2M^o} t^2 - \frac{\alpha}{M^o} t \right\} \quad (7)$$

Time independent ($\beta=0$) and dependent ($\beta \neq 0$) versions are both considered, as models 1a and 1b, respectively. Model 2 adds a further degree of freedom, by allowing the magma reservoir to expand or contract linearly with time. That is, $Q^{\text{in}} = \alpha^{\text{in}} + \beta t$ and $Q^{\text{out}} = \alpha^{\text{out}} + \beta t$ where the β parameters in each expression are equal. This corresponds to the case where the input and output fluxes differ by constant amounts. The rate of change of reservoir mass (or

Application of the model

Compositional variation in episode 3–31 lavas erupted from the Pu'u 'Ō'ō vent is thought to be controlled by the progressive mixing of an initial hybrid end member (magma A) with a new MgO-rich end member (magma B; Garcia et al. 1992), consistent with the two-component box-mixing model presented above. To test this hypothesis, the analytical mixing solutions defined by Eqs. (7) and (8) are fit to the geochemical mixing trend spanning these episodes. Lava compositional data are first converted into mass fractions of magma A and B (X_A and X_B). Model trends are optimized to match this dataset by varying the unknown model parameters: initial reservoir volume (M^o), input flux (α^{in} , β), and output flux (α^{out} , β). In turn, these parameters describe the Pu'u 'Ō'ō magmatic system during the mixing period.

The fraction of each magmatic component (X_A^{res} and X_B^{res}) is evaluated from the CaO/TiO₂ ratio of erupted lavas by defining initial and final end members and solving the standard hyperbolic mixing relationships for each sample (e.g., Langmuir et al. 1978). The CaO/TiO₂ ratio was chosen due to the high analytical precision of CaO and TiO₂ (0.03 and 0.005 wt%; Rhodes 1988), the large relative difference between CaO/TiO₂ in the two end members (~25%; Fig. 2), and the insensitivity of the ratio to olivine fractionation. Although the fractionation of clinopyroxene, plagioclase, or titanomagnetite would remove CaO or TiO₂ from the system, affecting the calculated end-member mass fractions, petrographic and geochemical evidence suggests that significant fractionation of these phases did not occur. Phenocrysts (>0.5 mm) of clinopyroxene and plagioclase are virtually absent after episode 6, and never represent >1.0 vol% of lavas (Garcia et al. 1992), whereas titanomagnetite is found only as a groundmass phase in episode 3–31 lavas. An absence of an Eu anomaly in all Pu'u 'Ō'ō lavas (including the most evolved lavas) indicates that plagioclase has neither

accumulated in nor been fractionated from the magma in significant amounts (Garcia et al. 2000). Furthermore, linear mass balance calculations indicate that lava compositions in episodes 3–31 are closely recreated through mixing of the two end members and only minor olivine fractionation (<5 wt%) without the need for clinopyroxene or plagioclase fractionation (Garcia et al. 1992). The use of highly incompatible trace element ratios to determine fractional magmatic components would remove the affect of any minor crystallization. However, these ratios proved too imprecise to tightly constrain the mixing relationships (see trace element data in supplementary electronic material at <http://www.springerlink.com/link.asp?id=100402>). The minor degree of olivine fractionation necessary to explain short-term compositional variations (<1–5 vol%) is also consistent with the previously stated assumption that crystal fractionation is not significant relative to the input and output flux ($Q^{\text{xtal}} < 5\%$ of Q^{in}).

End-member compositions were selected from analyzed lavas based on compositional and spatial criteria (Table 1). The initial hybrid end member erupted during episode 1 from the January 23rd vent, ~200 m west of the future site of Pu‘u ‘Ō‘ō (sample 1–054; Neal et al. 1988). The new MgO-rich end member was chosen as the most MgO-rich lava erupted during the first 31 episodes, as indicated by the whole-rock Mg number. This lava (sample 31–368) erupted during episode 31, 808 days after the eruption commenced. Despite their compositional differences, isothermal densities of the two basalts, determined using the MAGMA computer program “(<http://www-geo.lanl.gov/Wohletz/KWare.htm>)”, differ by <1.5%. Relative MgO contents indicate that the MgO-rich end member was ~60° hotter than the initial hybrid end member (Helz and Thornber 1987). Accounting for temperature variations,

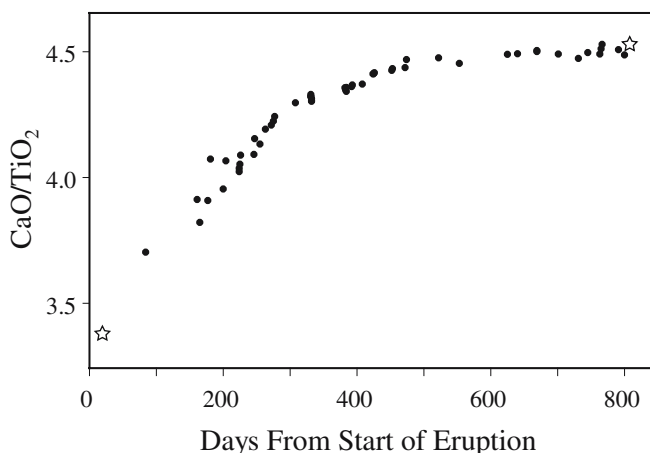


Fig. 2 Temporal variation of CaO/TiO₂ for episodes 3–31 lavas from the Pu‘u ‘Ō‘ō vent. Samples 1–054 (erupted during episode 1 from the adjacent 23 Jan vent) and 31–368 (*open stars*) are chosen as initial hybrid (magma A) and new MgO-rich (magma B) end members for mixing calculations. Lavas attain a nearly constant CaO/TiO₂ ratio by day 625, and maintain this ratio through episode 47 (day 1270) with minimal variations. Geochemical data from Garcia et al. (1989; 1992). Analytical precision (one sigma) is approximately equivalent to symbol size (Rhodes 1988)

Table 1 End-member lava compositions^a

Sample number	Initial magma (A)	Input magma (B)
	1–054	31–368
SiO ₂	50.33	49.56
TiO ₂	3.04	2.35
Al ₂ O ₃	13.74	12.55
Fe ₂ O ₃	12.74	12.39
MnO	0.17	0.18
MgO	6.12	9.47
CaO	10.26	10.62
Na ₂ O	2.50	2.17
K ₂ O	0.63	0.44
P ₂ O ₅	0.33	0.23
Total	99.86	99.96

^aCompositions are given in oxide wt% and are taken from Garcia et al. (1989; 1992)

the densities of the two magmas, as calculated by MAGMA, differ by <1.0%.

Non-linear expressions for the volume fraction of each magma in the reservoir as a function of time are defined in the MATLAB programming environment using Eqs. (7) and (8). Model input parameters (α^{in} , α^{out} , and β) are simultaneously optimized by minimizing the sum of the squares between the non-linear model and the data, using the MATLAB function `nlinfit`. The start of the mixing (t^{onset}) between evolved hybrid and MgO-rich end members is not directly observable. Garcia et al. (1992) speculated that mixing began as early as 8 days after the start of the eruption, based on a polynomial fit to the CaO/TiO₂ mixing trend. We test this prediction by optimizing the model over a range of values for t^{onset} , selecting the time that minimizes the root mean square (RMS) error between the model and the data. The start of mixing is restricted to a period between the propagation of a dike down the rift zone (day 0), triggering the eruption (Wolfe et al. 1987) and the eruption of the first recorded hybrid lava from mixing with the new MgO-rich magma (day 84). These constraints are consistent with the observed geochemical time series (Fig. 2). All reported times are relative to the start of the eruption (00:31 3 Jan 1983 Hawaiian standard time). Model results are dimensionally scaled to match the cumulative erupted volume of episode 3–31 lavas (Fig. 3).

Modeling results

Least-squares minimization converged for all four models, reproducing the observed mixing trend (Fig. 4). Residuals between data points and calculated mixing curves (due to minor crystal fractionation or imperfect mixing) are symmetrically distributed and do not indicate inconsistencies between the model and the data trend. Best-fit parameters and 95% confidence intervals on the parameters are presented in Table 2. All models fit the geochemical data equally well, as indicated by the negligible differences

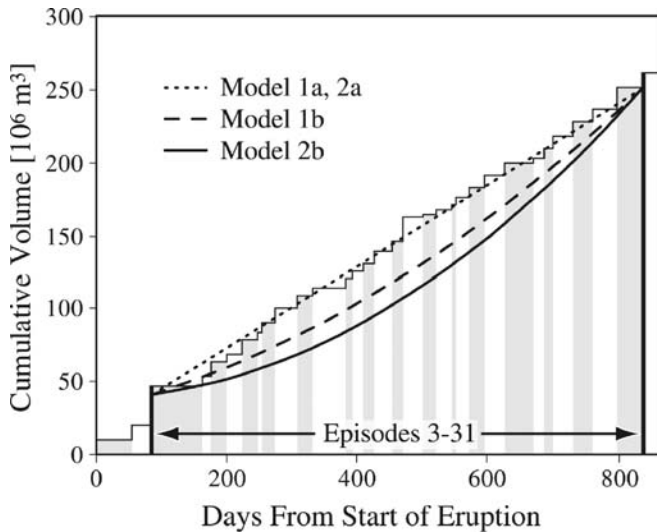


Fig. 3 Observed and calculated cumulative volumes of lava for episodes 1–32 of the Pu‘u ‘Ō‘ō eruption. The four model curves are scaled to match the cumulative volume of Pu‘u ‘Ō‘ō lavas (*stair-step pattern*) from episodes 3–31. Only ~14% of episode 3 lavas erupted from the Pu‘u ‘Ō‘ō vent; the remainder were evolved hybrid lavas erupted from the 1123 vent, 1.5 km down-rift (Wolfe et al. 1988). Alternating episodes (including repose periods) are shaded gray. Eruption volumes and dates from Wolfe et al. (1988) and Heliker and Mattox (2003)

between RMS errors (Table 2). Time dependent models (1b and 2b) have the lowest RMS errors. However, these models also predict an increase in eruption rate over time ($\beta^{\text{out}} > 0$), which conflicts with observed output fluxes (Fig. 3). Thus, we favor the time independent mixing models (1a and 2a). In both of these models, output flux is

constant over time and is constrained to equal the average eruption rate of the Pu‘u ‘Ō‘ō vent during episodes 3–31 (~0.28 million m^3/day ; Wolfe et al. 1988; Heliker and Mattox 2003). Models 1a and 2a predict initial magma reservoir volumes of 46 and 49 million m^3 , with 95% confidence intervals of ± 2 and ± 1 million m^3 , respectively. Model 2a predicts a smaller magma input than output, resulting in a decrease in reservoir volume with time ($dV/dt < 0$; Table 2), which was not observed (Hoffmann et al. 1990). The additional degree of freedom allowed by a variable reservoir volume decreases the RMS error only slightly (from 3.0 to 2.7%), and the magnitude of both dV/dt and the difference in V^o is relatively small.

Model results were evaluated using new XRF trace element data for episode 3–31 lavas (electronic supplementary material at <http://www.springerlink.com/link.asp?id=100402>). These data were obtained using a more precise instrument (Rhodes and Vollinger 2004) then was used previously (e.g., Garcia et al. 1992). Ratios of incompatible trace elements (e.g., Sr/Zr) provide a check on magma mixing models because these ratios are relatively insensitive to crystallization of the observed minerals (e.g., Albarède 1993). However, incompatible trace element ratio variations in the Pu‘u ‘Ō‘ō lavas are smaller and have larger analytical errors than CaO/TiO₂ (0.9% for Sr/Zr vs. 0.3% for CaO/TiO₂; Rhodes and Vollinger 2004). Nevertheless, the observed trace element ratios variations (Fig. 5) are consistent with our interpretations based on CaO/TiO₂ (Fig. 2). They support the proposed mixing model for compositional variation during episodes 3–31.

RMS errors are minimized when mixing begins shortly after the start of the eruption (day 0–34; Table 2). However, within the window of time considered, the specific onset of

Fig. 4 Results of fitting box-mixing models to Pu‘u ‘Ō‘ō geochemical data for episodes 3–31. Models 1a and 1b assume constant volume reservoirs; models 1a and 2a assume constant input and output fluxes over time. All curves fit the observed geochemical trends equally well. Best-fit fluxes and reservoir volumes are given in Table 2. Percent of MgO-rich component is calculated from CaO/TiO₂ ratios, using compositions for lava samples 1–054 and 31–368 as end members. Uncertainty due to analytical precision is approximately the size of the data points

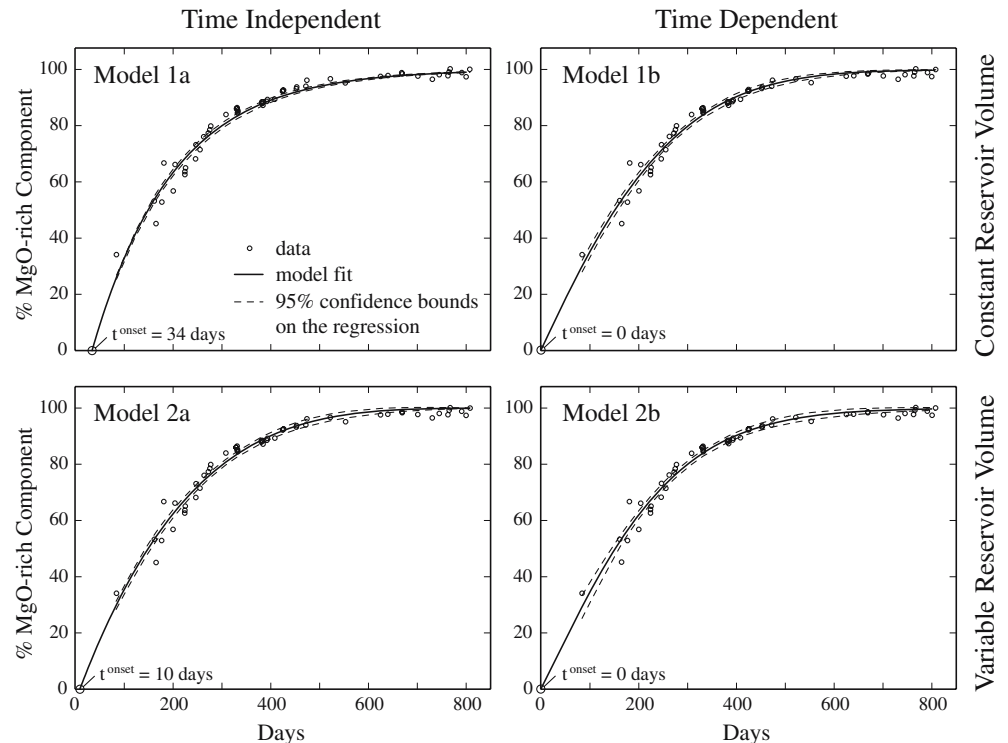


Table 2 Results of fitting geochemical mixing trend to non-linear analytical solutions

Best-fit parameters for analytical solutions ^a								Calculated magma chamber volume				
	α^{in}	+/- ^b	α^{out}	+/- ^b	β^{in}	+/- ^b	β^{out}	t^{onset}	RMS error ^c	V°	+/- ^b	dV/dt
	($10^6 \text{ m}^3/\text{day}$)				($10^3 \text{ m}^3/\text{day}^2$)			(days)		(10^6 m^3)		($10^6 \text{ m}^3/\text{day}$)
Constant volume magma chamber												
1a	0.28	(0.01)	$=\alpha^{\text{in}}$		0 ^d		0 ^d	34	3.0%	46	(2)	0
1b	0.14	(0.02)	$=\alpha^{\text{in}}$		0.37	(0.13)	$=\beta^{\text{in}}$	0	2.6%	36	(5)	0
Variable volume magma chamber												
2a	0.22	(0.02)	0.28	(0.01)	0 ^d		0 ^d	10	2.7%	49	(1)	-0.05
2b	0.10	(0.05)	0.06	(0.25)	0.58	(1.54)	$=\beta^{\text{in}}$	0	2.6%	28	ND	0.04

^aFluxes are defined as: $Q^{\text{in}}=\alpha^{\text{in}}+\beta^{\text{in}}t$; $Q^{\text{out}}=\alpha^{\text{out}}+\beta^{\text{out}}t$

^b95% confidence intervals on the parameters are calculated from model residuals and the Jacobian matrix

^cRoot mean square error between the mixing trend and modeled mixing curve, in percent MgO-rich component

^dThese parameters are constrained to be zero. *ND* not determined

mixing (t^{onset}) is poorly constrained by the mixing model. For example, delays in t^{onset} of ~30 days result in only a ~15–20% increase in the RMS error (to ~3.5%). The uncertainty associated with the onset of mixing does not greatly impact magma flux and reservoir volume predictions. In the extreme case, delaying t^{onset} ~30 days (to day 50) changes these values by <15% ($Q^{\text{in}} \sim Q^{\text{out}}=0.28$ million m^3/day , $V^{\circ}=42.3$ million m^3). Thus, the modeling cannot accurately constrain the date when mixing began.

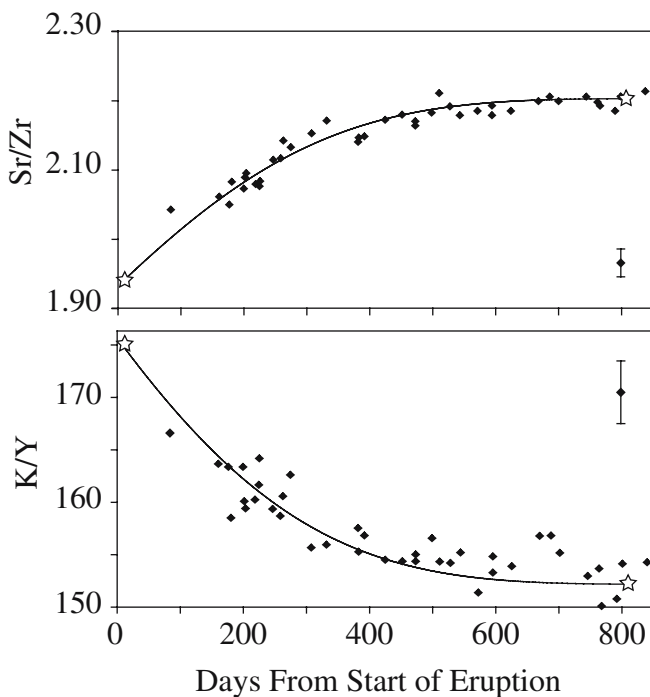


Fig. 5 Temporal variation in K/Y and Sr/Zr ratios for episode 3–31 lavas from the Pu‘u ‘Ō‘ō vent. Stars indicate end-member compositions. Curved lines are the predicted trace element ratios, based on the results of time independent variable volume reservoir model (2a). The new major and trace element data that was used to make these plots are available as electronic supplementary material at <http://www.springerlink.com/link.asp?id=100402>. Error bars show one sigma errors

Discussion

Magma plumbing configuration

Geochemical and geophysical observations suggest that the Pu‘u ‘Ō‘ō magmatic system includes three necessary components: an initial reservoir of evolved hybrid magma, an intruding dike of MgO-rich magma (Garcia et al. 1992), and a shallow dike-shaped reservoir below Pu‘u ‘Ō‘ō (Hoffmann et al. 1990). Two possible scenarios for magma movement between these storage components are: (1) mixing between the MgO-rich magma and the evolved hybrid magma in the core of the rift zone (~3–4 km depth; Wolfe et al. 1987), followed by injection of an intermixed magma into the shallow dike (Fig. 6), or (Fig. 2) simultaneous injection of separate batches of MgO-rich and evolved magmas directly into the shallow reservoir (Garcia et al. 1992). Several lines of evidence support the first of these scenarios. To produce the observed smooth, monotonic mixing trend, the timescale of compositional homogenization within the magma reservoir must be shorter than the typical period between episodes (20–30 days). However, systematic eruption of low-MgO lavas

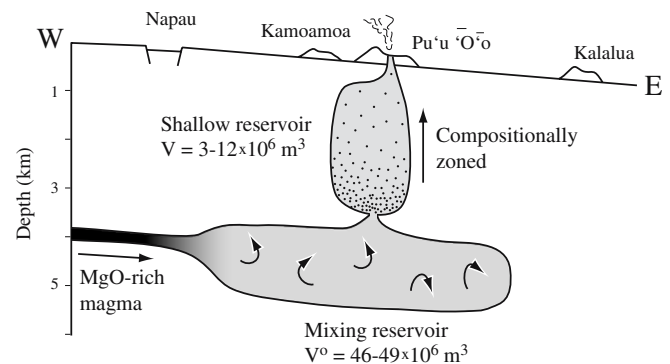


Fig. 6 Cartoon showing proposed geometry of Pu‘u ‘Ō‘ō magma reservoirs (after Garcia et al. 1992). Compositional variation during episodes 5–10, 30 and 31 suggests the shallow reservoir is compositionally zoned due to olivine fractionation and accumulation. The volume estimate for the shallow reservoir is from Hoffmann et al. (1990). No vertical exaggeration shown

followed by high-MgO lavas during several eruptive episodes (5–10, 30, 31) suggests the progressive emptying of a stratified magma reservoir (Garcia et al. 1992). These two observations indicate that the magma mixing and chemical zonation probably occurred in two separate reservoirs, as outlined above in the first scenario. Furthermore, scenario two requires systematically changing input fluxes of both evolved hybrid and MgO-rich magmas (Fig. 4). While this scenario is not impossible, the combination of two unsteady magma inputs is unlikely to induce the observed steady effusion rate (Fig. 3).

The mixing model described in this paper tests the feasibility of the first scenario (Fig. 6). The results from the modified box-mixing model, despite its inherent simplicity, demonstrate that a model built on robust mass balance relationships can recreate the observed geochemical trend. As shown in Eq. (7), a constant input of new magma paired with a constant output of well-mixed magma leads to an exponentially decaying fraction of original magma in the chamber. Therefore, the first scenario does not require physically improbable combinations of magma inputs (e.g., influx rate from two independent reservoirs producing a constant output and progressive compositional change; Figs. 2 and 5). While more complicated input (Q^{in}) and output (Q^{out}) flux functions (e.g., higher order polynomials) may also recreate the observed mixing trend, it is unlikely that they would yield a significantly lower RMS error than models 1 and 2 (Table 2).

In addition to supporting box model-type mixing, the geochemical modeling presented here demonstrates that the locus of magma mixing and the shallow dike are two distinct reservoirs. For time independent mixing models, the calculated initial volume of the evolved magma reservoir is ~46–49 million m^3 . If the reservoir volume is allowed to change with time (model 2a), it contracts by ~0.05 million m^3/day . In contrast, ground deformation studies indicate that the shallow dike reservoir was initially an order of magnitude smaller (~3 million m^3) and grew to only ~10–12 million m^3 by episode 10 (Hoffmann et al. 1990). The difference in initial reservoir volumes and the change in volumes over time indicate that the shallow dike-shaped reservoir did not store the initial volume of evolved hybrid magma. Instead, the two reservoirs are separate but necessary components of the proposed Pu‘u ‘Ō‘ō magmatic system (Fig. 6). Intermixed magmas from the larger mixing reservoir refilled a shallow dike-like body rapidly during the eruption and more slowly during repose periods (Hoffmann et al. 1990). The deformation signal of the larger reservoir may have been obscured by the frequent inflations and deflations of the shallow reservoir. Olivine fractionated in the shallow dike forming a smaller volume of fractionated magma (<17 million m^3 ; Garcia et al. 1992).

Rift zone magma storage

A minimum estimate for the volume of magma stored in the rift zone prior to the Pu‘u ‘Ō‘ō eruption is provided by combining (1) the volume of evolved hybrid magma

initially contained in the mixing reservoir (~46–49 million m^3) and (2) the volume of evolved hybrid magma erupted during episodes 1, 2, and part of 3 that is not included in mixing calculations (~42 million m^3 ; Wolfe et al. 1988). Additionally, an unknown volume of magma solidified in the system during the ~2 years of mixing. Therefore, at least ~90 million m^3 of magma may have been stored in Kīlauea’s rift zone before the Pu‘u ‘Ō‘ō eruption.

Historic eruptions of evolved lavas along the east rift zone of Kīlauea, interpreted as having tapped reservoirs within the rift zone (e.g., Wright and Fiske 1971), offer comparative estimates of magma storage. Volumes of evolved lavas erupted during the first stages of the 1955 eruption (~44 million m^3 ; Macdonald and Eaton 1964; Wright and Fiske 1971) and the 1977 eruption (~35 million m^3 ; Moore et al. 1980) are nearly half the estimated volume of magma storage prior to the Pu‘u ‘Ō‘ō eruption. However, these volume estimates do not include unerupted magmas, which may have solidified or erupted at a later date (e.g., episodes 1–3 of the Pu‘u ‘Ō‘ō eruption probably tapped unerupted magma from the 1977 eruption; Garcia et al. 1992). Thus, the sizes of rift zone magma reservoirs along Kīlauea’s active east rift zone associated with twentieth century eruptions are significant, as suggested by seismic studies (Klein et al. 1987).

Conclusions

Mixing between stored rift zone magmas and intruding MgO-rich magmas, as observed in the 1960 and early Pu‘u ‘Ō‘ō eruptions, is a common process in Kīlauea rift zone eruptions. A two component box-mixing model is proposed to describe the early Pu‘u ‘Ō‘ō magma system and an analytical expression is derived for the fraction of each component in the magma chamber at any given time. This simple model reproduces the observed geochemical mixing trend. When constrained by observed lava effusion rates, the model predicts an initial reservoir volume of 46 ± 2 million m^3 if the reservoir volume is constant and 49 ± 1 million m^3 if the reservoir volume is allowed to change over time. Three lines of evidence differentiate this mixing reservoir from the shallow dike-shaped reservoir directly below Pu‘u ‘Ō‘ō suggested by ground deformation measurements: (1) the observed monotonic mixing trend requires the mixing time to be shorter than the typical repose period between episodes, whereas the systematic MgO variation in erupted lavas in episodes 5–10, 30, and 31 suggests that the shallow reservoir is compositionally zoned prior to eruption, (2) the volume of the mixing reservoir is much larger than the initial volume of the dike-shaped reservoir (~3 million m^3), and (3) geochemical modeling does not indicate a marked increase in reservoir size with time (i.e., to six times the original volume), as suggested by modeling surface deformation. These observations have led us to propose a two-reservoir system with a ‘mixing reservoir’ and a shallow, dike-shaped reservoir where crystal fractionation was prevalent. Mixing may take place within the rift zone in the reservoir that

stored the evolved hybrid magmas formed during episode 1 of the Pu'u 'Ō'ō eruption.

Acknowledgements We would like to acknowledge F. Albarède and A. Pietruszka for their thoughtful comments on a draft of this paper, and J. Hammer for her input throughout the entire project. Mahalo to the staff of the USGS Hawaiian Volcano Observatory for providing access to samples and sharing data, especially E. Wolfe and G. Ulrich, and to J.M. Rhodes and M. Vollinger for high-quality XRF data. This paper is based upon work supported by the National Science Foundation under Grant No. 0336874. This paper is SOEST contribution No. 6793.

References

- Albarède F (1993) Residence time analysis of geochemical fluctuations in volcanic series. *Geochim Cosmochim Acta* 57:615–621
- Albarède F (1995) Introduction to geochemical modeling. Cambridge University Press, Cambridge, pp 543
- Broecker WS (1974) Chemical oceanography. Harcourt, New York, pp 214
- Faure G (1986) Principles of isotope geology. Wiley, New York, pp 589
- Flinders J, Clemens JD (1996) Non-linear dynamics, chaos, complexity and enclaves in granitoid magmas. *Trans R Soc Edinburgh Earth Sci* 87:217–224
- Garcia MO, Ho RA, Rhodes JM, Wolfe EW (1989) Petrologic constraints on rift-zone processes: results from episode 1 of the Pu'u 'Ō'ō eruption of Kīlauea Volcano, Hawaii. *Bull Volcanol* 52:81–96
- Garcia MO, Rhodes JM, Wolfe EW, Ulrich GE, Ho RA (1992) Petrology of lavas from episodes 2–47 of the Pu'u 'Ō'ō eruption of Kīlauea Volcano, Hawaii: evaluation of magmatic processes. *Bull Volcanol* 55:1–16
- Garcia MO, Pietruszka AJ, Rhodes JM, Swanson K (2000) Magmatic processes during the prolonged Pu'u 'Ō'ō eruption of Kīlauea Volcano, Hawaii. *J Petrol* 41:967–990
- Hawkesworth CJ, George R, Turner SP, Zellmer G (2004) Time scales of magmatic processes. *Earth Planet Sci Lett* 218:1–16
- Heliker CC, Mattox TN (2003) The first two decades of the Pu'u 'Ō'ō-Kūpaianaha eruption: chronology and selected bibliography. *US Geol Surv Prof Pap* 1676:1–28
- Helz RT, Thornber CR (1987) Geothermometry of Kīlauea Iki lava lake, Hawaii. *Bull Volcanol* 49:651–668
- Hildreth W, Moorbath S (1988) Crustal contributions to arc magmatism in the Andes of central Chile. *Contrib Mineral Petrol* 98:455–489
- Hoffmann JP, Ulrich GE, Garcia MO (1990) Horizontal ground deformation patterns and magma storage during the Pu'u 'Ō'ō eruption of Kīlauea Volcano, Hawaii: episodes 22–42. *Bull Volcanol* 52:522–531
- Klein FW, Koyanagi RY, Nakata JS, Tanigawa WR (1987) The seismicity of Kīlauea's magma system. *US Geol Surv Prof Pap* 1350:1019–1185
- Langmuir CH, Vocke J, Robert D, Hanson GN (1978) A general mixing equation with applications to Icelandic basalts. *Earth Planet Sci Lett* 37:380–392
- Macdonald GA, Eaton JP (1964) Hawaiian volcanoes during 1955. *US Geol Surv Bull* 1171:170
- Moore RB, Helz RT, Dzuris D, Eaton GP, Koyanagi RY, Lipman PW, Lockwood JP, Puniwai GS (1980) The 1977 eruption of Kīlauea Volcano, Hawaii. *J Volcanol Geotherm Res* 7:189–209
- Neal CA, Duggan TJ, Wolfe EW, Brandt EL (1988) Lava samples, temperatures, and compositions. *US Geol Surv Prof Pap* 1463:99–126
- Perugini D, Poli G, Mazzuoli R (2003) Chaotic advection, fractals and diffusion during mixing of magmas: evidence from lava flows. *J Volcanol Geotherm Res* 124:255–279
- Pietruszka AJ, Garcia MO (1999) The size and shape of Kīlauea Volcano's summit magma storage reservoir: a geochemical probe. *Earth Planet Sci Lett* 167:311–320
- Rhodes JM (1988) Geochemistry of the 1984 Mauna Loa eruption: implications for magma storage and supply. *J Geophys Res* 93:4453–4466
- Rhodes JM, Vollinger MJ (2004) Composition of basaltic lavas sampled by phase-2 of the Hawaii Scientific Drilling Project: geochemical stratigraphy and magma types. *Geochem Geophys Geosyst* 5:Q03G13, DOI:10.1029/2002GC000434
- Wolfe EW, Garcia MO, Jackson DB, Koyanagi RY, Neal CA, Okamura AT (1987) The Pu'u 'Ō'ō eruption of Kīlauea Volcano, episodes 1 through 20, January 3, 1983, to June 8, 1984. *US Geol Surv Prof Pap* 1350:471–508
- Wolfe EW, Neal CA, Banks NG, Duggan TJ (1988) Geologic observations and chronology of eruptive events. *US Geol Surv Prof Pap* 1463:1–98
- Wright TL, Fiske RS (1971) Origin of the differentiated and hybrid lavas of Kīlauea Volcano, Hawaii. *J Petrol* 12:1–65